Физика и техника полупроводников, 2012, том 46, вып. 7

Synthesis and characterization of the as-deposited $Cd_{1-x}Pb_xS$ thin films prepared by spray pyrolysis technique

© *M. Kamruzzaman*[¶], *R. Dutta*[*], *J. Podder*[+]

Department of Physics, Begum Rokeya University,
Rangpur-5400, Bangladesh
[*] Department of Physics, City University,
Dhaka-1213, Bangladesh
[+] Department of Physics, Bangladesh University of Engineering and Technology,
Dhaka-1000, Bangladesh

(Получена 30 ноября 2011 г. Принята к печати 26 декабря 2011 г.)

$Cd_{1-x}Pb_xS$ thin films were prepared by spray pyrolysis technique onto glass substrate at 300°C temperatures. The prepared films were characterized elemental, structural and optical properties by energy dispersive X-ray, scanning electron microscopy, X-ray diffraction and UV-VIS spectrophotometer. Energy dispersive X-ray confirmed the presence of Cd, S and Pb in the films. SEM images show that the deposition covered the substrate well uniformly and incorporation of Pb. Crystal stucture was found hexagonal and the estimated grain size was lies in between 9 to 49 nm. The optical band gap was decreased from 2.43 to 2.07 eV.

1. Introduction

In recent years, much effort has been given on CdS semiconductor for making $p{-}n$ heterojunction thin solar cells. Heterojunction cells are attracting a great deal of attention because of their much fold importance in a wide spectrum of optoelectronic devices [1]. CdS is a hexagonal closed packed structure and has a wide band gap of 2.43 eV, low resistivity and high transparency in the visible range [2]. Several authors have been doped CdS with a wide variety of elements (F, Pt, Pb, Zn, Al, Co, In, Sn, etc.) to meet the demands of several application fields such as thin film solar cells [2], electrochemical cells [3], gas sensor [4] and it has also been employed in high efficiency solar cells formed with Cu_2S [5], $Cu(InGa)Se_2$ [6] etc. At present most of the semiconductors research is dedicated towards the fabrication of low-sized particles and these particles/semiconductor show a large optical band gap when the crystallite size becomes less than the Bohr exciton radius [7–9]. On the other hand PbS belonging to IV–VI group semiconductor with a direct narrow band gap (0.41 eV) suitable for infrared detection applications [10,11]. It is also used as a photo resistance, laser diode, humidity and temperature sensors, decorative coatings and solar control coatings [12–15]. The band gap of CdS has been tailored by mixing it with lead (Pb) ions [16]. As CdS and PbS are highly sensitive to light and in view of their practical application, a study of their mixed thin films structure as spray pyrolysis converters is of technical importance [17].

For the preparation CdS and Pb doped CdS thin films a variety of deposition techniques have been used such as, chemical bath deposition [18], aqueous synthesis [19], precipitation technique [20], quenching method [21] etc. Spray pyrolysis deposition technique have been considered as a viable technique for production of Pb doped CdS thin films due to its many advantages over the conventional methods, viz., low cost experimental set up, high spatial selectivity, precise control over maneuvering the impurity concentration and possibility to overcome the solubility limit. This method is convenient for papering pinhole, homogeneous, smoother thin films with the required thickness. It provides an easy way to dope any element in a ratio of required proportion through the solution medium. In addition, this technique could be used for the production of large scale area for thin film deposition without employing any high vacuum system [22].

$Cd_{1-x}Pb_xS$ have been synthesized by spray pyrolysis technique and studied their elemental, surface morphological, optical and electrical properties by energy dispersive X-ray, scanning electron microscope, X-ray diffraction and UV-VIS spectrophotometer.

2. Experimental

Fig. 1 shows the typical experimental setup for the preparation of $Cd_{1-x}Pb_xS$ thin films by the spray pyrolysis method. Aqueous solution of 0.1 M cadmium acetate, $Cd(CH_3COO)_2 \cdot 3H_2O$, 0.2 M thiourea ($NH_2CSNH_2$) and 0.1 M lead acetate, $Pb(CH_3COO)_2 \cdot 2H_2O$ were taken as sources of Cd, S and Pb. A considerable amount of (100 ml) solution was taken in the Beaker „F“ fitted with the spray nozzle „A“. The clean substrate with a suitable mask (2.5×2 cm) was put on the susceptor of the heater „H“. The distance between the tip of the nozzle and the surface of the glass substrate was kept 25 cm. The substrate temperature was kept at 523 K and was measured by placing a copper constantan thermocouple on the substrate.

When compressed air of carried gas is passed through „P“ (at 0.50 bar pressure) a vacuum is created at the tip of the nozzle to suck the solution from the tube after which the spray starts and the spraying solution was automatically carried to the reactor zone upto 5 min where film was deposited onto the heated substrate. About $1.5\,cm^3/min$

[¶] E-mail: mkzaman_phybuet@yahoo.com

Table 1. Atomic % for different compositions of $Cd_{1-x}Pb_xS$ thin films

Concentration, x	E_g (eV)	Element	Atomic percentage (%) by EDAX analysis	Atom % error	Total
$x = 0$	2.43	Cd	54.79	±1.62	100.00
		S	45.21	±1.25	
$x = 0.05$	2.36	Cd	54.34	±3.84	100.00
		S	44.56	±2.39	
		Pb	1.11	±1.37	
$x = 0.10$	2.25	Cd	52.70	±2.42	100.00
		S	44.68	±1.67	
		Pb	2.62	±0.95	
$x = 0.15$	2.17	Cd	52.74	±3.11	100.00
		S	43.22	±1.72	
		Pb	4.04	±0.79	
$x = 0.20$	2.07	Cd	54.98	±2.45	100.00
		S	39.91	±1.35	
		Pb	5.11	±0.61	

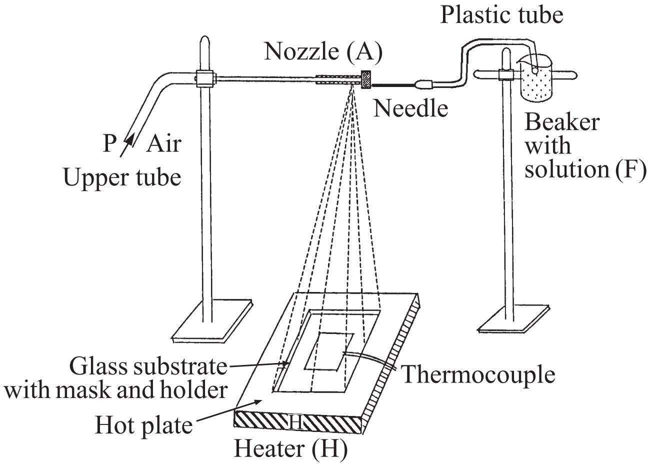

Figure 1. Experimental set up of spray pyrolysis method.

spray rate through the nozzle to ensures a uniform thickness of the films. In the hot-zone, the atomized solution is dried and the constituent metal salts decompose and form intimate $Cd_{1-x}Pb_xS$ films. Various parameters like air pressure, deposition rate, distance between tip of the nozzle to substrate, cooling rate etc. affect the physical, electrical and optical properties of the films. So all these parameters were keep constant throughout to deposit the all films. The possible chemical reaction may take place on the heated substrate as follows:

$$Cd_{1-x}(CH_3COO)_2\cdot 3H_2O + Pb_x(CH_3COO)_2\cdot 2H_2O$$
$$+ NH_2CSNH_2 \frac{523\,K}{\text{Decompose}} \rightarrow Cd_{1-x}Pb_xS + NH_3\uparrow$$
$$+ NH_4\uparrow + 7CO_2\uparrow + 4CH_4\uparrow + 2H_2\uparrow + \text{Steam}\uparrow .$$

2.1. Characterization

The thicknesses of the films were measured by the setup of Fizeau fringes method at the department of Physics, BUET. The elemental and surface morphology of the films were taken by energy dispersive X-ray (EDX) and scanning electron microscopy (SEM) setup (Inspect IS50 FEI Company). The X-ray diffraction (XRD) of as deposited films were taken by using a molybdenum CuK_α ($\lambda = 1.54178$ Å), radiation diffractometer, PHILIPS model „X'Pert PRO XRD System". The optical absorbance and transmittance spectra were taken at room temperature with respect to plain glass substrate using double beam UV-VIS spectrophotometer (UV-1601PC Shimadzu, Japan) in BCSIR, for wavelength 380 to 1100 nm.

3. Results and discussion

3.1. Compositional Studies

The quantitative analysis of the films is shown in Table 1. There are two peaks observed for $x = 0$ that corresponds to Cd and S and confirms the CdS film. For $x = 0.05$, 0.10, 0.15 and 0.20 there have some extra peaks of Pb in the spectra. It is worth to mention that the as-deposited films are of $Cd_{1-x}Pb_xS$. Cd peak height decreases with increasing Pb indicates the incorporation of Pb into the system. From Table 1 it is evident that for all the films the amounts of Cd, S and Co are present but the as deposited films are non-stoichiometric in composition. EDX analysis shows that the films are cadmium reach. It may be due to the fact that the reactivity of cadmium is more than sulphur ions [23]. The deviation in the composition can be adjusted by changing the volume or concentration or both of the individual ion sources in the reaction mixture.

Table 2. Lattice constants, volume, c/a ratio and grain size of $Cd_{1-x}Pb_xS$ thin films

Concetration, x	Lattice constants		Volume of CdS (Å^3)	c/a	Grain size for (002) peak (nm)
	a (Å)	c (Å)			
$x = 0.00$	4.136	6.708	99.384	1.622	9.132
$x = 0.05$	4.139	6.722	99.724	1.623	49.061
$x = 0.10$	4.137	6.728	99.578	1.623	45.646
$x = 0.15$	4.145	6.718	99.993	1.621	49.062
$x = 0.20$	4.137	6.713	99.474	1.623	19.344

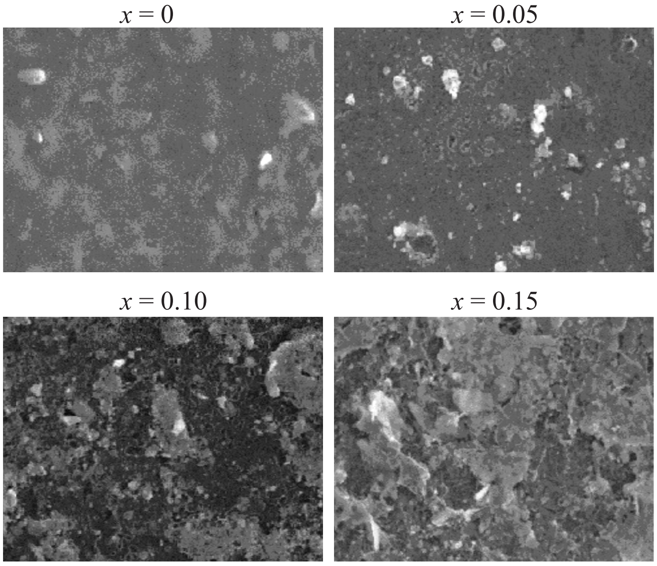

Figure 2. SEM images under 10 000 magnifications of $Cd_{1-x}Pb_xS$ films for $x = 0$, 0.05, 0.10 and 0.15.

3.2. Surface Morphology

Surface morphology under 10 000 magnifications of the as deposited films is shown in Fig. 2. The deposited films are polycrystalline in nature and deposition covers the substrate well. In as-deposited states the film was very dense with no observable voids or pinholes. The films have less defined grain boundaries under this magnification. For pure CdS there is no precipitation of Pb but for $x = 0.05$, 0.10, and 0.15 Pb precipitation is observed.

3.3. X-ray diffraction (XRD)

X-ray diffraction (XRD) has been taken of as-deposited films by using molybdenum K_α radiation diffractometer. There are four different fundamental peaks is observed in Fig. 3 (for $x = 0$, 0.05, 0.10 and 0.15) which are identified as (100), (002), (101) and (110) planes matched with standard JCPDS data card 80−0006 of CdS hexagonal crystal structure. But for $x = 0.20$ two extra peaks are arises. At higher concentration excess S exist in the form of elemental S arising from the extraneous decomposition of S ions [24]. The lattice parameters (a and c) were estimated for (100) and (002) planes using the relation (1)

$$\frac{1}{d_{hkl}} = \left[\frac{4}{3}\frac{(h^2 + hk + k^2)}{a^2} + \frac{l^2}{c^2}\right]^{1/2}. \tag{1}$$

The estimated lattice parameters a and c, volume, c/a ratio and grain size are presented in Table 2. From Table 1 it is found that the values of a and c are nearly constant with Co content and the average c/a ratio close to 1.62. So our synthesized films are wurttzite hexagonal structure. These results imply that the Pb^{2+} has been substituted into the crystal lattice of CdS. As the ionic radius of Pb^{2+} (1.18 Å) larger than that of Cd^{2+} (0.97 Å), thus Pb^{2+} ions substituted into the crystal lattice of CdS and brought distortion in CdS lattice. The estimated lattice parameters are very close to the standard value. Grain size of the prepared films was estimated for the stronger peak (002) using Scherrer formula (2)

$$D_g = \frac{0.9\lambda}{\Delta \cos\theta} \tag{2}$$

where D_g is the average grain size, λ is the wavelength of the radiation used as the primary beam of K_α ($\lambda = 1.54178$ Å), θ is the angle of incidence in degree and Δ is the full width at half maximum (FWHM) of the peak in radian, which was determined experimentally after correction of instrumental broadening (in the present case it is 0.05°). Average grain size of films lies between 49

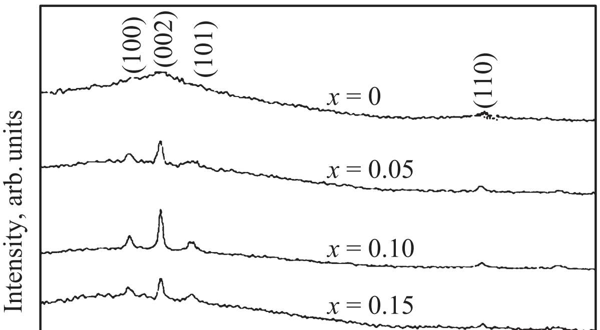

Figure 3. XRD spectra of $Cd_{1-x}Pb_xS$ as deposited thin films.

and 9 nm which indicate the nanometric size of CdS grains developed in the film.

3.4. Optical Properties

The optical transmittance (T) behavior of the films is shown in Fig. 4 within the wavelength range 380 to 1100 nm. All the films demonstrate more than 60% transmittance at wavelengths higher than 700 nm. A sharp fall of the transmittance is observed between the wavelength 550 to 600 nm, which is due to the strong absorbance of the films in this region. The over all T decreases with the increasing incorporation of Pb in the solution. The direct band gap energy of the films were determined from the intercept on the energy axis after extrapolation of the straight line section of $(\alpha h\nu)^2$ vs. $h\nu$ curve (Fig. 5). Band gap (E_g) of the films decreases from 2.43 to 2.07 eV, which indicated that small amount incorporation of Pb greatly affects on the optical band gap. This variation of the band gap energy may be useful to design a suitable window material in fabrication for solar cells [25].

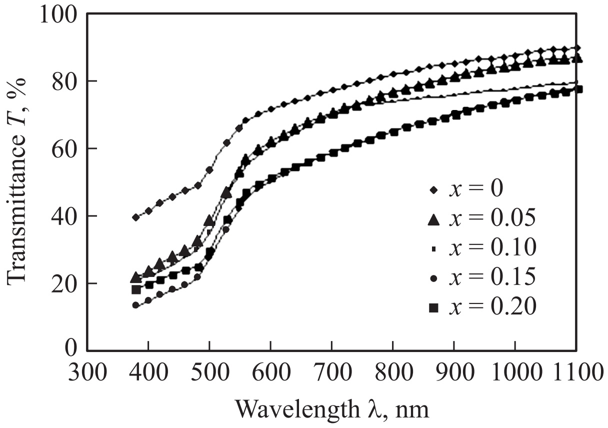

Figure 4. Variation of the optical transmittance with wavelength of $Cd_{1-x}Pb_xS$ films.

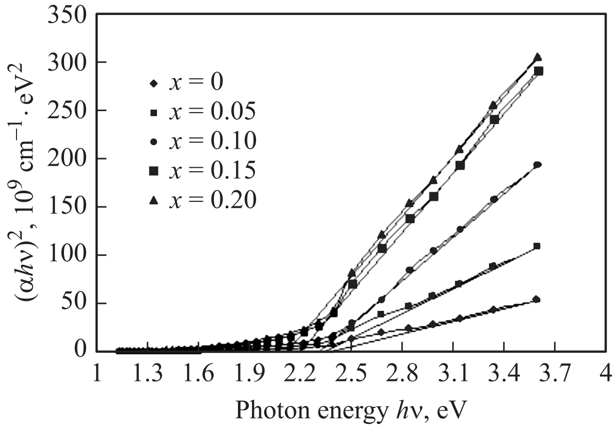

Figure 5. Variation of band gap with photon energy for $Cd_{1-x}Pb_xS$ as deposited films.

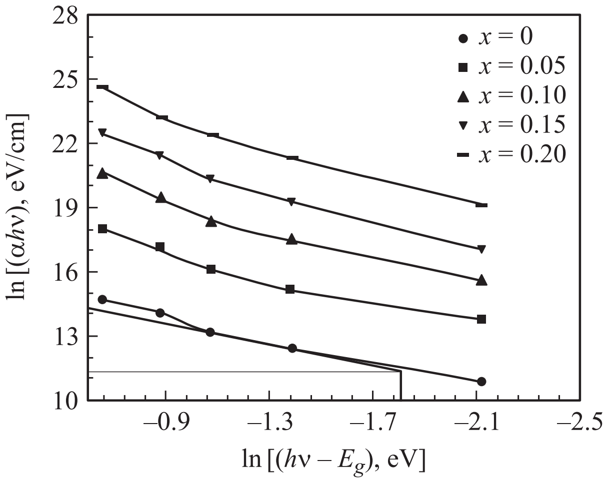

Figure 6. Determination of the nature of the band gap.

The optical transmission spectra of these films were taken to evaluate the absorption coefficient (α), band gap energy (E_g) and nature of transition involved. The theory of optical transmission gives the relationship between the absorption coefficient (α) and the photon energy $(h\nu)$ as

$$\alpha h\nu = A(h\nu - E_g)^n \tag{3}$$

where α is the absorption coefficient, $h\nu$ is the photon energy, E_g is the optical band gap and A is the constant which is related to the effective masses associated with the valance band and the conduction band. The n assumes values of 1/2, 2, 3/2 and 3 for allowed direct, allowed indirect, forbidden direct and forbidden indirect transitions, respectively. For allowed direct type of transitions

$$\alpha h\nu = A(h\nu - E_g)^{1/2}. \tag{4}$$

The modes of optical transitions in these films have been determined by Pal et al. [27]. and Eq. 4 can be rearranged as

$$\ln(\alpha h\nu) = \ln A + n\ln(h\nu - E_g). \tag{5}$$

The plot of $\ln(\alpha h\nu)$ versus $\ln(h\nu - E_g)$ (Fig. 6) is a straight line whose slope gives the power factor n and the results of above analysis for typical samples and the calculated values of n for all the films are listed in Table 3. The obtained values of n suggest that the fundamental absorption edge in the films is formed by the direct allowed transition.

Table 3. Calculated power factor n of the $Cd_{1-x}Pb_xS$ thin film structures

Composition, x	Values of power factor, n
$x = 0.00$	0.404
$x = 0.05$	0.454
$x = 0.10$	0.418
$x = 0.15$	0.523
$x = 0.20$	0.403

4. Conclusions

Energy dispersive X-ray confirmed the presence of Cd, S and Pb compositions in the films. SEM images under 10 000 magnifications could not revealed any specific grain size or grain boundary but shows deposition cover the substrate well. The as deposited films are polycrystalline nature with wurtzite hexagonal structure. The optical studies exhibit that the direct band gap strongly dependent on the concentration x. The optical band gap is varied from 2.42 to 2.07 eV which is required for solar cell and optoelectronic device applications. The transmittance spectra showed 60% transmission for all the films above 700 nm wavelength.

The authors are would like to thank Dr. Dilip Kumar saha chief Scientific officer BAECD for his cordial support in performing XRD and Mr. Uddin Ahmed Science officer, BCSIR for SEM and EDX measurements. The authors are also thankful to Bangladesh University of Engineering and Technology (BUET) for financial support.

References

[1] A. Ashour. J. Optoelectron., Adv. Mater., **8** (4), 1447 (2006).
[2] M.D. Archbold, D.P. Halliday, K. Durose, T.P.A. Hase, D. Smyth-Boyle, K. Govender. *1 st IEEE Photovoltaic Specialists Conf.* (*Lake Buena Vista FL*), (2005) p 476.
[3] M. Ristova, M. Ristov. Sol. Energy Mater. Solar Cells **53**, 102 (1998).
[4] U.S. Jadhav, S.S. Kale, C.D. Lokhande. Mater. Chem. Phys., **69**, 25 (2001).
[5] T. Kanemitsu, T. Nagai, T. Kushida, S. Nakamura, Y. Yamada, Y. Taguchi. Appl. Phys. Lett., **80**, 267 (2002).
[6] R.B. Hall, J.B. Meakin. Thin Sol. Films, **63**, 203 (1979).
[7] T. Nakoda, N. Okano, Y. Tanaka, A. Kunioka. *Proc. 1st World Conf. on Photovoltaic Energy Conversion* (Hawaii, 1994).
[8] C.B. Murray, C.R. Kagan, M.G. Bawendi. Science, **270**, 1335 (1995).
[9] N. Mathur, K. Joshi, Rakesh, G.V. Subbaraju, H.K. Sehgal. Physica E, **23**, 56 (2004).
[10] H. Kanazawa, S. Adachi. J. Appl. Phys., **83**, 5997 (1998).
[11] R.K. Joshi, A. Kanjilal, H.K. Sehgal. Appl. Surf. Sci., **221**, 43 (2004).
[12] S. Kumar, Z.A. Khan, M.A.M. Khan, M. Hussain. Current Appl. Phys., **5**, 561 (2005).
[13] I. Pop, C. Nascu, V. Lonescu, E. Indvea, I. Bratu. Thin Sol. Films, **307**, 240 (1997).
[14] P.K. Nair, M.S.T. Nair, A. Frenandez, M. Ocampo. J. Phys. D: Appl. Phys., **22**, 829 (1989).
[15] J.J. Valenzuela, R. Ramirez, A. Mendoza, M. Sotelo. Thin Sol. Films, **441**, 104 (2004).
[16] M.A. Barote, A.A. Yadav, R.V. Suryawanshi, E.U. Masumdar. J. Ovonic Res., **7** (3), 45 (2011).
[17] K.L. Chopra, S. Major, D.K. Panday. Thin Sol. Films, **102**, 1 (1983).
[18] M.A. Barotea, A.A. Yadavb, L.P. Deshmukh, E.U. Masumdarb. J. Non-Oxide Glasses, **2**, 151 (2010).
[19] L.Y. Chieh, S.Ch. Kan. ICCE-18 (July 4–10, 2010, Anchorage, Alaska, USA).
[20] K. Sanjeev, B. Bhattacharya. Indian J. Pure, Appl. Phys., **43**, 609 (2005).
[21] T.C. Harmann. *Mass. Inst. Technol. Lincoln Lab.*, **3**, 10 (1971).
[22] M. Bedir, R. Kayali, M. Oztas. Turk. J. Phys., **26**, 121 (2002).
[23] G.S. Shahane, B.M. More, C.B. Rotti, L.P. Deshmukh. Mater. Chem. Phys., **47**, 263 (1997).
[24] Y. Ueno, H. Kaigawa, T. Ohashi, T. Sugiura, H. Minoura. Sol. Energy Mater., **15**, 421 (1987).
[25] A. Goswami. *Thin Film Fundamentals. New Age International Publications* (New Delhi, India, 1996). p. 279.

Редактор Т.А. Полянская